Eclética Química Journal

Original article
iq.unesp.br/ecletica

| Vol. 44 | n. 4 | 2019 |

Rapid and selective extraction of trace amount of Pb(II) in aqueous samples using a magnetic ion-imprinted polymer and detection by flame atomic absorption spectrometry

Saeed Babaee+, Seyed Ghorban Hosseini, Mohammad Mirzaei

Faculty of Chemistry and Chemical Engineering, Malek Ashtar University of Technology, Iran.

+Corresponding author: Saeed Babaee, Phone: +98 2122987672, email address: safnba@gmail.com

ARTICLE INFO

Article history:
Received: March 12, 2019
Accepted: June 26, 2019
Published: October 1, 2019

Keywords:
1. extraction
2. magnetic
3. ion imprinting polymer
4. lead
5. n-benzoyl-n-phenyl hydroxylamine

ABSTRACT: A magnetic Pb(II) ion-imprinted polymer was synthesized using magnetic Fe_3O_4@SiO_2 nanospheres as supporter, n-benzoyl-n-phenyl hydroxylamine as ligand, 4-vinyl pyridine as monomer, ethylene glycol dimethacrylate as crosslinker and 2,2′-azobis(isobutyronitrile) as the initiator. The template was removed from the polymer using 4 mL of HCl (2 mol L^{-1}). The chemical structure, morphology-particle size, elemental analysis, thermal behavior and magnetic properties of the sorbent were evaluated using Fourier-transform infrared spectroscopy, scanning electron microscopy & ImageJ software - Energy dispersive X-ray system, thermal gravimetric analysis and vibrating sample magnetometry. Various parameters such as pH, equilibrium extraction time, temperature and the eluent were optimized. The results showed the sorbent adsorption capacity was 92.3 mg g^{-1} in pH 6.0 media, equilibrium time of 7 min at 40 °C. Calibration linearity was 2-150 µg L^{-1} with detection limit of 0.3 µg L^{-1}. The prepared sorbent had high selectivity and was successfully applied to the removing of lead in real samples.

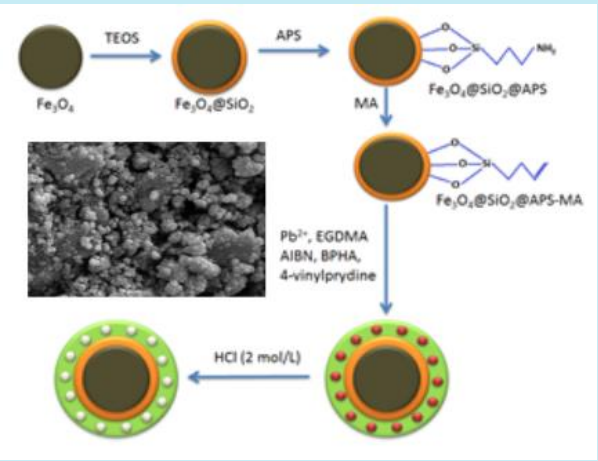

1. Introduction

It is clear that heavy metals contamination represents serious hazards to the ecosystem and especially to humans because of the complex toxicological effects on living beings[1]. Lead has been accepted as an important toxic heavy metals resulting from mining, acid battery factories[2], metal plating[3], printing[4], textile[5], photographic materials[6], ceramic and glass industries as well as explosive manufacturing[7]. Through the joined system of water–plant–animal–human, Pb(II) is transferred into human body and causes to various severe health problems in vital organs of humans, such as damage to kidney, liver, blood composition, central nervous system (CNS) due to binding sites on cerebellar phosphokinase C at trace amounts and also retarding the reproductive system in mental function[8-10]. The maximum permitted amount of lead ions by world health organization (WHO) in drinking water fixed as 10.0 µg L^{-1} and for the U.S. environmental protection agency (USEPA) is 15.0 µg L^{-1} [11]. Consequently, the developments of reliable and highly sensitive techniques to the determination and then removal of lead in water samples as the pollutant sources are crucially necessary.

Nowadays flame atomic absorption spectrometry (FAAS) because of its analytical abilities has been confirmed for trace analysis of

metal ions but lead concentration in environmental waters is usually lower than FAAS detection limit[12]. Therefore, a separation and enrichment pretreatment is necessary before to Pb(II) determination at the μg L^{-1} levels. Several methods have been developed for Pb^{2+} ions separation-preconcentration, such as liquid–liquid extraction[13], liquid-phase microextraction[14], solid phase extraction (SPE)[15], coprecipitation[16] and cloud point extraction[17] which among them SPE is more common due to the higher enrichment factor, minimal costs, environment friendly and simple automation.

Different solid phases have been applied as sorbents which among them, molecularly imprinted polymers (MIPs) have been widely utilized for selective separation of organic and also inorganic compounds from aqueous samples[18]. Similar sorbents to MIPs are ion imprinted polymers (IIPs) that produced by chelating metal ions with the relevant ligands and then polymerizing with a monomer. Ion imprinted polymers (IIPs) are more attractive for separation of inorganic ions due to their high selectivity, high preconcentration factor and chemical stability[19]. In this manner Liu[20] synthesized a surface-imprinted mesoporous sorbent for Pb(II) ion by the post-synthesis method and the adsorption capacity reached to 36.6 mg g^{-1}. Ghoohestani[21] synthesized Pb(II)-IIP by polymerization of chitosan on the surface of MCM-41 with adsorption capacity of 57.7 mg g^{-1}. Fan[22] synthesized silica-supported sorbent functionalized with Schiff base by coupling a surface imprinting technique with a sol–gel process for removal of Pb(II) ions with adsorption capacity of 54.9 mg g^{-1}.

In present study, a novel magnetic Pb-IIP containing of n-benzoyl-n-phenyl hydroxylamine was synthesized on the surface of Fe_3O_4@SiO_2 by a surface imprinting technique for the selective and efficient preconcentration of lead ions in various aqueous samples. The adsorption experiments coupled with FAAS system was used to the analyte quantification at μg L^{-1} levels.

2. Materials and methods

2.1 Reagents and materials

Ferric chloride, sodium acetate, ammonium hydroxide and tetraethyl orthosilicate (TEOS) were used for synthesis of Fe_3O_4@SiO_2 nanoparticles and for the functionalization. Triethylamine (TEA) and 3-aminopropyltriethoxysilane (APS) were applied for the preparation of the imprinted polymer, utilized from 4-vinyl pyridine (VP), n-benzoyl-n-phenyl hydroxylamine (BPHA), ethylene glycol dimethacrylate (EGDMA), maleic anhydride (MA) and α, α'-azobisisobutyronitrile (AIBN). $Pb(NO_3)_2$ were used as source of Pb(II). Stock solutions were prepared daily from Pb^{2+} standard solution of 1000.0 mg L^{-1} by serial dilutions. Other chemicals were provided from Merck Company (Darmstadt, Germany). Deionized water was used for preparation of all solutions.

2.2 Apparatus

The measurements were performed using flame atomic absorption spectrometer (Varian, Model Spectra A-20 Plus) with hollow cathode lamp (10 mA current, spectral bandwidth and wavelength of 0.5 and 283.3 nm respectively). The infrared spectra of the IIP samples were obtained using a Shimadzu 8400S FTIR spectrometer. A scanning electron microscopy along with ImageJ software (Ver. 5.1.1)-energy dispersive X-ray (Joel-JSMT 300A) were used for morphology-particle size-elemental analysis. TGA studies were carried out with Stanton Redcroft-STA-780 system applying heating rate of 10 C min^{-1} in a temperature range of 50-600 °C, under air atmosphere with a flow rate of 50 mL min^{-1}. Magnetic properties were analyzed using a vibrating sample magnetometer (Microsense-EZ VSM). The pH was determined using a Metrohm pH meter (M. Lab-827) with a combined glass–calomel electrode.

2.3 Synthesis of magnetic nanospheres (MNSs)

The MNS was synthesized by a solvothermal reduction method[23]. Typically, 1.35 g $FeCl_3.6H_2O$ was dissolved in ethylene glycol (40 mL) to form a clear solution, followed by the addition of sodium acetate (3.6 g) and polyethylene glycol (1.0 g). The mixture was vigorously treated by ultrasonic bath for 30 min. After that it was refluxed at 180 °C for 8 h, and then allowed to cool down to room temperature. The black product was washed several times with ethanol and deionized water. Then it was dried at 60 °C for 6 h.

Eclética Química Journal, vol. 44, n. 4, 2019, 73-84
ISSN: 1678-4618
DOI: 10.26850/1678-4618eqj.v44.4.2019.p73-84

2.4 Synthesis of SiO_2 coated MNSs (Fe_3O_4@SiO_2)

These nanospheres were prepared according to a previously reported method with minor modifications[24]. Typically, 0.5 g of the MNS was dispersed in 60 mL ethanol and 10 mL of deionized water, and treated by sonication for 15 min, followed by the addition of 1.0 mL ammonium hydroxide (25%) and 3.0 mL TEOS sequentially. The mixture was reacted for 12 h at room temperature under continuous stirring. The resultant product was collected by an external magnetic field and rinsed six times with ethanol and water. Subsequently, 8.0 g Fe_3O_4@SiO_2 were mixed with 100 mL of HCl (2 mol L^{-1}) and refluxed for 6h. the activated microspheres were recovered and washed several times. Finally, the obtained activated Fe_3O_4@SiO_2 was dried under vacuum at 60 °C for 3 h.

2.5 Synthesis of functional Fe_3O_4@SiO_2 microspheres

Two grams of Fe_3O_4@SiO_2 activated microspheres were added to 50 mL of anhydrous toluene, followed by an addition of moderate TEA and 12 mL APS. The mixture was incubated at 110 °C for 12 h in nitrogen atmosphere. Then the Amino modified microspheres (Fe_3O_4@SiO_2-APS) were magnetically separated, rinsed with toluene and vacuum dried at 25 °C. To prepare the Fe_3O_4@SiO_2-APS-MA particles, 1.5 g Fe_3O_4@SiO_2-APS and 2.5 g MA were added to 50 mL DMF, then the mixture reacted for 24 h at room temperature. The solid separated with magnetic field, rinsed with DMF and ethanol and then dried under vacuum at 25 °C for 2 h.

2.6 Synthesis of Pb^{2+} imprinted-polymer magnetic adsorbent (MIIP)

First, 2 mmol of $Pb(NO_3)_2$ was dissolved in 25 mL DMF under ultrasonic oscillation. Then 4 mmol BPHA, 8 mmol 4-vynil pyridine and 25 mL methanol were added to the solution and stirred overnight at room temperature[25]. After that, 0.5 g Fe_3O_4@SiO_2-APS-MA, 8 mmol EGDMA and 0.1 g AIBN were added to the solution and reacted at 60 °C for 24 h under nitrogen atmosphere. The final product was collected with magnetic field and washed with DMF and methanol. The lead ions in polymer were removed by an HCl solution (2 mol L^{-1}). The removal of the template was determined by FAAS. Schematic diagram of this procedure is shown in Fig. 1.

Magnetic non-ion imprinted polymer (MNIIP) were prepared by same process exception of $Pb(NO_3)_2$ addition for the purpose of contrast test.

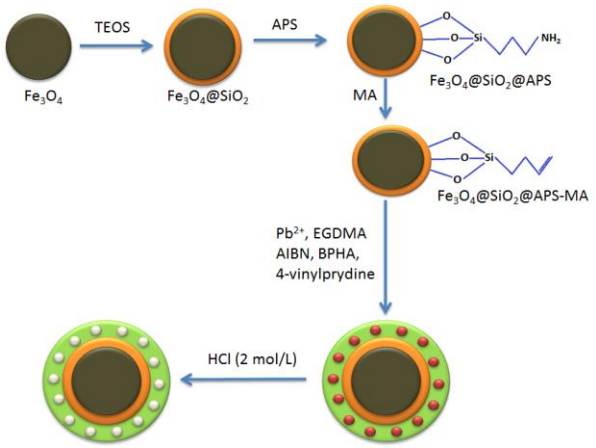

Figure 1. A schematic diagram for synthesis of magnetic IIP.

2.7 Determination procedure

The pH of sample solution containing Pb(II) was adjusted to 6 by drop-wise additions of 0.1 mol L^{-1} of NaOH or HCl. Then 0.2 g of the sorbent was added into 100 mL of the solution and shake for 7 min via 40 °C. After adsorption equilibrium, these magnetic nanoparticles were separated by a magnet and the adsorbed Pb^{2+} ions were eluted with 4 mL HCl (2 mol L^{-1}) for 15 min. Now, the analyte in the supernatant and the eluent were determined by FAAS.

Percent extraction of lead (E%) and adsorption capacity (q) of magnetic ion-imprinted polymer (MIIP) was calculated via the following formulas (Eq. 1 and 2):

$$E\% = 100\ (C_i - C_e) / C_i \quad (1)$$

$$q = (C_i - C_e)\ V/m \quad (2)$$

Where: C_i (mg L^{-1}) and C_e (mg L^{-1}) are the Pb^{2+} concentrations before and after adsorption in the solution respectively. V (L) is the volume of added solution, m (g) is the mass of MIIP in dry form.

2.8 Sample preparation

Environmental and wastewater samples were collected from Tehran, Polur (Anahita Co.) and an ammonium perchlorate factory in Iran respectively.

Eclética Química Journal, vol. 44, n. 4, 2019, 73-84
ISSN: 1678-4618
DOI: 10.26850/1678-4618eqj.v44.4.2019.p73-84

Prior to sampling, the bottle was cleaned with deionized water, diluted nitric acid and deionized water in succession. The samples were filtered through a cellulose filter membrane (0.45 µm) and their pH was adjusted before the determination.

3. Results and discussion

3.1 Characterization of MIIP

3.1.1 Structure investigation with FT-IR

The FT-IR spectra of Fe_3O_4@SiO_2 and MIIP showed in Fig. 2. The peak at 1150 cm^{-1} is corresponding to Si-O-Si stretching that observed in both of samples, which indicates SiO_2 is encapsulated correctly inside the MIIP. The carbonyl peak at 1730 cm^{-1}, O-H peak at 3205 cm^{-1} and C-N peak at 1450 and 1380 cm^{-1} showed the presence of ligand (BPHA) in the MIIP structure.

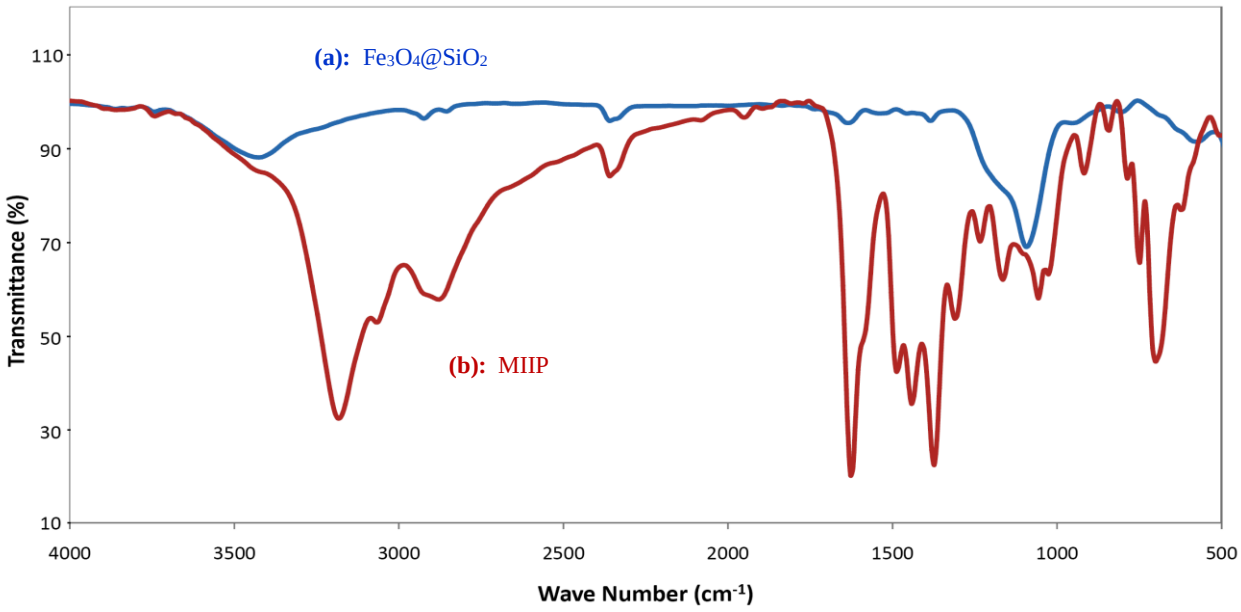

Figure 2. FT-IR spectra of (a) Fe_3O_4@SiO_2 and (b) MIIP.

3.1.2 Morphology analysis

The morphology and particle size histograms of the synthesized adsorbents were analyzed via SEM system and ImageJ software. The results of the MNIIP and MIIP nanoparticles are shown in Fig. 3(a, b). SEM image of Fig. 3a shows a homogenous and smooth surface for MNIIP nanospheres with particle size range of 30-40 nm that obtained from ImageJ software usage. As shown in SEM image of Fig. 3b, in the presence and then removing of Pb(II), a porous structure was resulted for MIIP which was attributed to imprinted cavities. This rough structure of this surface on the surface of MIIP is favor to mass transfer and the formation of three-dimensional recognition sites. In this manner the particle size range of MIIP was obtained 20-30 nm.

Eclética Química Journal, vol. 44, n. 4, 2019, 73-84
ISSN: 1678-4618
DOI: 10.26850/1678-4618eqj.v44.4.2019.p73-84

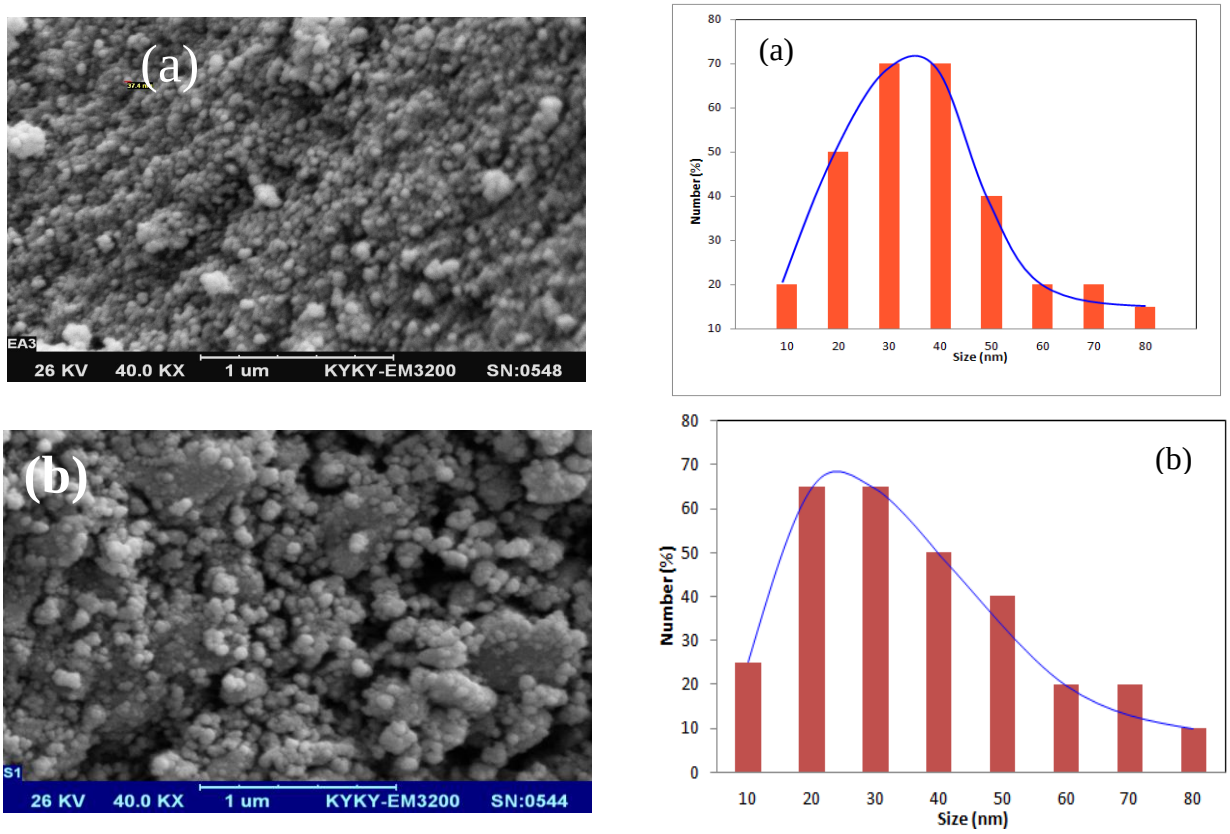

Figure 3. The SEM-Particle size analysis of MNIIP (a) and MIIP (b) adsorbents.

3.1.3 Elemental analysis

The EDX spectrums of MIIPs after adsorption and then elution of Pb(II) are shown in Fig. 4(a, b) respectively. As seen in Fig. 4a the spectrum of the no leached MIIP revealed that significant amount of the analyte was adsorbed in the sorbent from the initial solution. Also Fig. 4b related to the leached MIIP confirmed the elimination of lead in the sorbent after rinsing with the selected eluent.

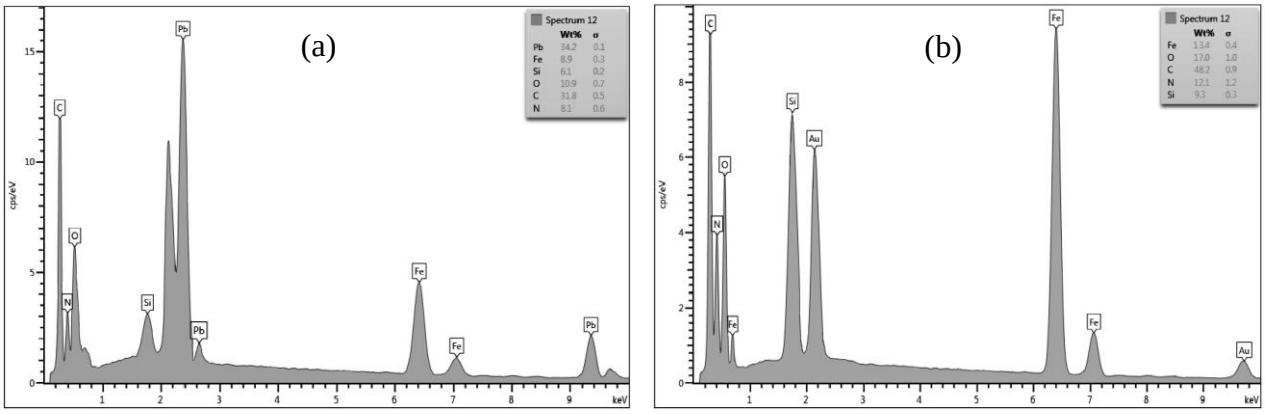

Figure 4. The EDX spectrums of the no leached (a) and leached (b) MIIPs.

3.1.4 Thermal studies by TGA

The amount of materials that modified the surface of nanoparticles can be valued by TGA. The TGA behavior of Fe_3O_4@SiO_2 and MIIP are shown in Fig. 5. The thermogram in Fig. 5a shows that the Fe_3O_4 has good thermal stability up to 500 °C with only a little loss of about 3.9%. As shown in Fig. 5b, when the temperature was changed from 280 to 350 °C, a 72.3% reduction in

Eclética Química Journal, vol. 44, n. 4, 2019, 73-84
ISSN: 1678-4618
DOI: 10.26850/1678-4618eqj.v44.4.2019.p73-84

weight of MIIP resulted that might be due to the decomposition of organic materials such as APS and polymeric layer. Hence, the results demonstrated the formation of an imprinted polymer. The remaining weight thermogram of MIIP can be attributed to Fe_3O_4 particles with higher thermal stability. The amount of capsulated Fe_3O_4@SiO_2 in MIIP is 23.8% that is appropriate for showing magnetic properties.

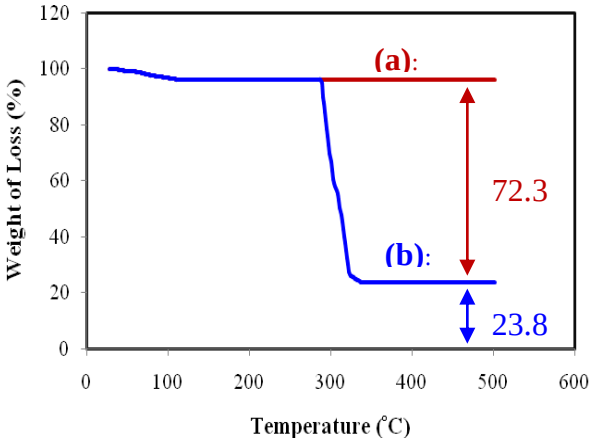

Figure 5. TGA thermograms of (a): Fe_3O_4@SiO_2 and (b): MIIP.

3.1.5 Magnetism analysis

The magnetic properties of the, Fe_3O_4@SiO_2, Pb(II)-MIIP and Fe_3O_4 were characterized using vibrating sample magnetometry (VSM) technique in the magnetic field of -10,000 to +10,000 Oersted at 25 °C. As shown in Fig. 6, the hysteresis curve of these samples is fully reversible that means nanomaterials have superparamagnetic properties and could be easily and quickly separated from a suspension. The saturation magnetization value of Fe_3O_4, Fe_3O_4@SiO_2 and MIIP was about 59, 23 and 9 emu g^{-1}, respectively. The value of saturation magnetization was decreased by increasing modifying steps. The decrease in magnetization value can be attributed to the existence of IIP on the surface of the Fe_3O_4@SiO_2 nanoparticles. Also, this relationship can be seen in the comparison between Fe_3O_4@SiO_2 and Fe_3O_4. However, the MIIP with less magnetite encapsulation possesses enough magnetic response to meet the need of magnetic separation.

Also, from inset of Fig. 6, it is seen that in the absence of an external magnetic field, a yellow homogeneous dispersion was existed. When an external magnetic field was applied, the yellow particles were attracted to the wall of vial in a short time (about 50 s).

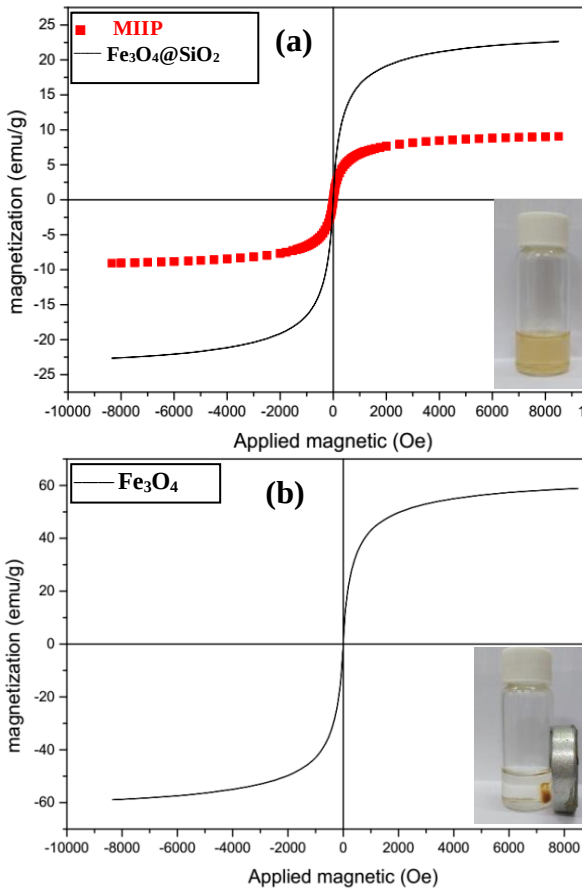

Figure 6. VSM curves of Fe_3O_4@SiO_2, MIIP (a) and Fe_3O_4 (b) at 25 °C.

3.2 Optimization of extraction conditions

Adsorption of Pb(II) from solution was performed in a batch method. Effects of media pH, eluent solvent (type, volume and concentration), adsorption-desorption time, and equilibrium temperature were studied. Adsorbent addition was set to 0.2 g in 100 mL solution and initial Pb(II) concentration was 1 mg L^{-1}. After adsorption equilibrium, the adsorbent was separated by external magnetic field and the analyte quantities in the eluents were determined by FAAS.

3.2.1 Effect of media pH

The solution pH is one important parameter that can effect on metal ion adsorption. In order to figure out of pH effect on Pb(II) adsorption, variety of pH were studied in the range 3.0 to 8.0. For prevention from sedimentation, increasing pH not

Eclética Química Journal, vol. 44, n. 4, 2019, 73-84
ISSN: 1678-4618
DOI: 10.26850/1678-4618eqj.v44.4.2019.p73-84

continued and the results are illustrated in Fig. 7. The results show that with the increase of pH to 6.0, percent recovery continually increased and then decreased. Probably the pH effects on functional groups of IIP or the chemistry of Pb^{2+} ions. At lower pH than 6.0 and presence of higher concentration of H^+, the active sites of the MIIP become protonated and their abilities for interaction with Pb(II) decreased. By increasing pH more than 6.0, Pb^{2+} ions can react by hydroxyl groups and the adsorption process would be decreased.

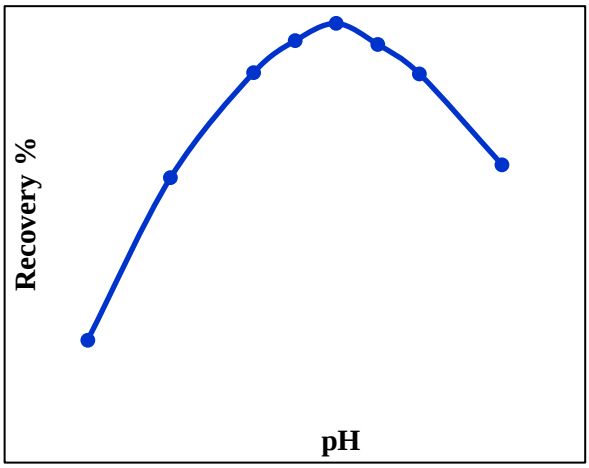

Figure 7. Effect of pH on the Pb^{2+} extraction. Condition: Pb initial concentration = 1 mg L^{-1}, adsorbent = 0.2 g, adsorption time = 7 min, desorption time = 15 min and T = 40 °C.

3.2.2 Selection of eluent solvent

To achieve the eluent for complete Pb(II) removing from MIIP, a series of commercial solutions of HNO_3 2 mol L^{-1}, HCl 2 mol L^{-1}, acetic acid (HOAC) 2 mol L^{-1}, HOAC-HCl (2:1 mol L^{-1}), HNO_3-HOAC (2:1 mol L^{-1}) were studied. As shown in Fig. 8a, HCl is the best eluent that can extract Pb(II) ions from MIIP. In the next step, diverse concentrations of HCl were investigated and as it can be seen in Fig. 8b, the best solution is HCl 2 mol L^{-1}. In the last section of eluent optimization, the volume of it optimized and as shown in Fig. 8c, 4 mL of HCl 2 mol L^{-1} was chosen as optimum condition of eluent for the experiments.

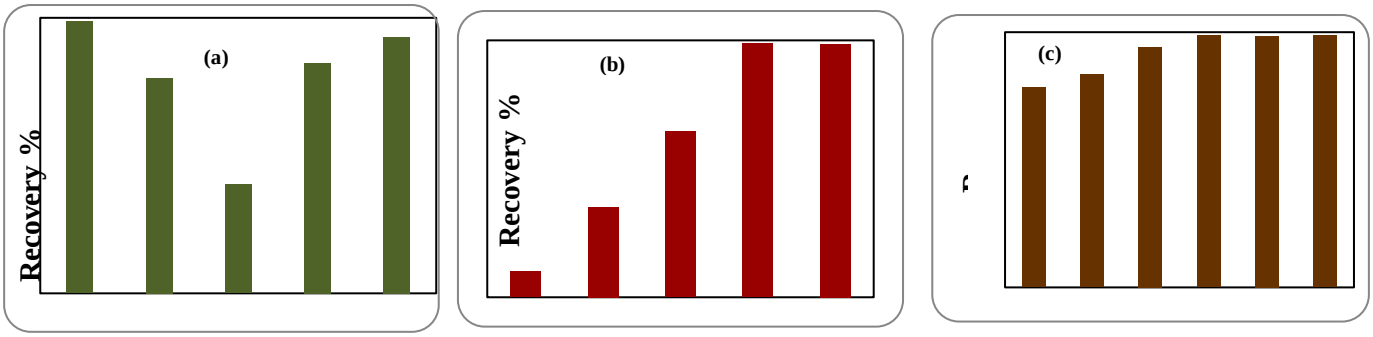

Figure 8. Effect of the eluent on the Pb^{2+} removing from MIIP, (a) Type; (b) Concentration; (c) Volume. Condition: Pb initial concentration = 1 mg L^{-1}, adsorbent = 0.2 g, pH 6.0, adsorption time = 7 min, desorption time = 15 min and T = 40 °C.

3.2.3 Effects of adsorption-desorption times

The adsorption and desorption times for Pb(II) were investigated under optimized conditions. As shown in Fig. 9a, it appears that MIIP showed good performance in adsorption during first 5 min and reached to equilibrium after 7 min and excess time does not provide any significant change in recovery. This time, probably due to plenty cavities that imprinted on the surface of thin MIIP that provide low diffusion resistance, is reliable and it can be stated that the process has fast equilibrium.

For desorption time optimization, different times (1-21 min) were studied and as it can be seen from Fig. 9b, optimum time is 15 min and this time was used in further experiments.

Eclética Química Journal, vol. 44, n. 4, 2019, 73-84
ISSN: 1678-4618
DOI: 10.26850/1678-4618eqj.v44.4.2019.p73-84

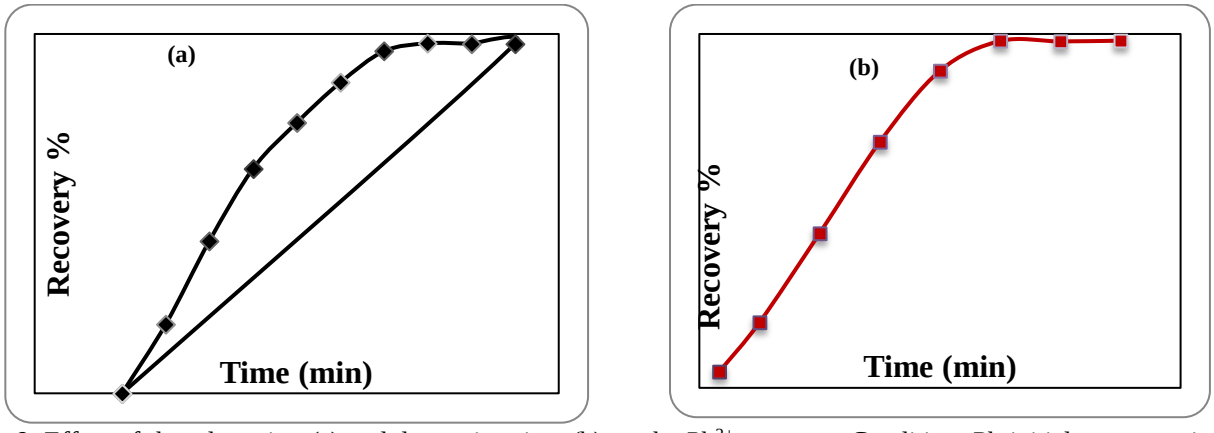

Fig. 9. Effect of the adsorption (a) and desorption time (b) on the Pb^{2+} recovery. Condition: Pb initial concentration = 1 mg L^{-1}, adsorbent = 0.2 g, pH 6.0 and T = 40 °C.

3.2.4 Effect of equilibrium temperature

In IIP techniques temperature has a noticeable effect on the adsorption behavior and analyte recovery. The effect of equilibrium temperature on the extraction behavior of Pb(II) on MIIP was shown in Fig. 10. As shown by increasing temperature from 25 to 40 °C, the recovery yield is increased thermodynamically. It can be seen that Pb(II) extraction in the range of 40 to 50 °C drastically decreased. This manner may be related to swelling of polymer. Probably in elevated temperature the size and geometry of cavities will be changed and could not be suitable for adsorption of Pb^{2+} as target ions.

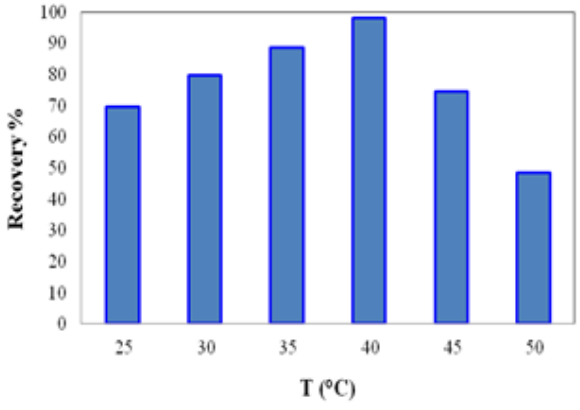

Figure 10. Effect of temperature on the Pb^{2+} recovery yield. Condition: Condition: Pb initial concentration = 1 mg L^{-1}, adsorbent = 0.2 g, pH = 6.0, adsorption time = 7 min, desorption time = 15 min.

3.3 Maximum adsorption capacity

For determination of maximum adsorption capacities of the ion imprinted polymer and nonimprinted polymers, 50 mg of each sorbents separately placed in a solution of 200 mgL^{-1} Pb(II) in pH 6.0 and the quantity of adsorbed ions were determined in both initial and eluent solutions. From three replicates, sorption capacities of MIIP and NIIP were calculated of 92.3 and 21.3 mg g^{-1} respectively. The results showed that MIIP compare to NIIP have a higher adsorption capacity for lead ions.

3.4 Analytical characteristics

Table 1 summarizes the analytical characteristics of the MIIP under the optimal conditions. The LOD of the proposed method was determined by 7 times placing of 0.2 g MIIP in 100 mL blank solutions and it was obtained to 0.3 µg L^{-1}. The precision (RSD, %) for 7 replicate uptaking of 10 μgL^{-1} Pb(II) was 2.4%. Also, the linear dynamic range of the calibration curve was obtained in 2-150 µg L^{-1} range.

Table 1 Analytical characteristics of the proposed extraction.

Regression Equation (n= 11)	$A_{283.3\ nm}$ = 0.0041 $C_{Pb\ (\mu gL^{-1})}$ + 0.002
Regression coefficient (r)	0.9994
Limit of detection [a] (μgL^{-1})	0.3
Reproducibility [b] (RSD, %)	2.4
Linear range (μgL^{-1})	2-150
[a] For 7 replicate runs of the blank (*n* = 7). [b] For 7 replicate measurements of 10 µg L^{-1} lead.	

Table 2 showed a comparison between the presented work and some others for preconcentration of lead (II). As seen the analytical

Eclética Química Journal, vol. 44, n. 4, 2019, 73-84
ISSN: 1678-4618
DOI: 10.26850/1678-4618eqj.v44.4.2019.p73-84

merits of the proposed method (e.g. adsorption time, adsorption capacity, detection limit and precision) are comparable and in general it is better than with those published reports. The main advantages of this method are more adsorption capacity and lower LOD.

Table 2 Comparison of some lead IIP sorbents performance with this work.

Sorbent type (monomer/crosslinker)	Ligand	Adsorption time (min)	Adsorption Capacity (mg g^{-1})	pH	LOD (ng mL^{-1})	R.S.D. (%)	Ref.
MIIP (MAA/EGDMA)	Salicyl Aldoxime	250	81.83	6	Note reported	Note reported	26
IIP (AAPTS/TEOS)	-	35	19.61	7.5	Note reported	Note reported	27
MIIP (VDPC/EGDMA)	DPC	12	68.1	7	1.3	2.9	28
IIP (4-VB-18-Crown-6/EGDMA)	4-VB-18-Crown-6	60	27.95	6	Note reported	Note reported	29
IIP (Acrylamide/NNMBA)	AA	20	42	5	0.34	2.1	30
MIIP (VDPA/EGDMA)	DPA	3	76.3	6	0.7	3.3	31
IIP (4-VP/EGDMA)	4-(2-Pyridylazo) Resorcinol	5	9.8	6	0.9	3.4	12
IIP (2-VP/EGDMA)	2-Amino Pyridine	90	85.6	5	0.75	2.7	32
IIP (2-VP/EGDMA)	Diphenyl Carbazone	5	75.4	6	0.42	2.1	33
MIIP (MAA/EGDMA)	-	4	51.8	7	1.7	4.1	34
MIIP (VPyDA/EGDMA)	APDC	4	55.89	7	0.9	1.8	35
MIIP (4-VP/EGDMA)	BPHA	7	92.3	6	0.3	2.4	This work

MAA: MethAcrylic Acid, EGDMA: Ethylene Glycol Dimethacrylate, AAPTS: 3-(2-aminoethyl Amino)Propyl Trimethoxy Silane, TEOS: Tetra Ethyl Ortho Silicate, VDPC: Vinyl-Di Phenyl Carbazide, DPC: Di Phenyl Carbazide, 4-VB-18-C-6: 4-Vinyl Benzo-18-Crown-6, NNMBA: N,N'-Methylene Bisacryl Amide, AA: Alginic Acid, VDPA: Vinyl Di Pyridyl Amine, DPA: Di Pyridyl Amine, 4-VP: 4-Vinyl Pyridine, 2-VP: 2-Vinyl Pyridine, VPyDA: 4-(Vinylamino)Pyridine-2,6-Dicarboxylic Acid, APDC: 4-Amino Pyridine-2,6-Dicarboxylic, BPHA: n-Benzoyl-n-Phenyl Hydroxyl Amine.

3.5 Effect of interfering ions

In order to prove specific recognition of magnetic ion imprinted polymer towards Pb(II) in the presence of common interfering ions, the selectivity of the prepared MIIP was investigated in binary systems[36]. The competitors examined were Na^+, K^+, Co^{2+}, Ni^{2+}, Ca^{2+} and Mg^{2+}. In this approach, each interfering ion was added to 100 mL of 10 µg L^{-1} Pb(II) solution under optimum conditions. After preconcentration by MIIP, the tolerable amount of each ion was determined separately. The tolerable amount is defined as the maximum concentration that could cause a change of less than 5% in signal compared to the initial signal of Pb^{2+} uptaking without any interference. As shown in Table 3, this Pb-MIIP have high selectivity in the existence of Co^{2+}, Ni^{2+}, Ca^{2+} and Mg^{2+} that probably was obtained in order to the use of BPHA as a new ligand.

Table 3 The tolerance limit of common interfering cations for Pb(II) determination.

Interfering ions	Tolerable concentration ratio (M:Pb)	Recovery %
Na^+	4000	99
K^+	4000	99
Co^{2+}	1500	98.1
Ni^{2+}	1500	97.9
Ca^{2+}	2000	96.8
Mg^{2+}	2000	95.3

3.6 Method application

The proposed procedure was applied for determination of lead content in two environmental samples and a waste water (from an ammonium perchlorate factory) solution. The amounts of Pb(II) ions were determined in the final eluents and the results are listed in Table 4. As seen, the mean recoveries for different spiking of Pb^{2+} are in the range 96.6-99.7%. Therefore, the proposed MIIP can be applied for the determination of lead in various samples.

Eclética Química Journal, vol. 44, n. 4, 2019, 73-84
ISSN: 1678-4618
DOI: 10.26850/1678-4618eqj.v44.4.2019.p73-84

Table 4 Recovery and precision of the determination of lead in various aqueous samples.

Samples [a]	Pb concentration (μgL^{-1})		
	Added	Found [b]	Recovery (%)
Tap water	-	Not detected	-
	5.0	4.8 ± 0.1	97 ± 3
	15.0	14.9 ± 0.8	99 ± 2
Mineral water	-	Not detected	-
	10.0	9.73 ± 0.09	97 ± 3
	30.0	29.90 ± 0.06	100 ± 2
Wastewater [b]	-	8.3	-
	5.0	13.1 ± 0.1	98 ± 3
	10.0	18.2 ± 0.7	100 ± 2
	20.0	28.2 ± 0.5	100 ± 2
[a] Sample description as described in the text.			
[b] Average of three determinations ± standard deviation			

4. Conclusions

In this research a new magnetic ion imprinted polymer (IIP@Fe_3O_4@SiO_2-APS-MA) for Pb^{2+} target was prepared by combination of surface imprinting technique and magnetic separation. The polymer synthesis and its characterization were proved by FT-IR, SEM-ImageJ, EDX, TGA and VSM techniques. The adsorption experiments combined to FAAS system showed that this sorbent have good analytical characteristics and high selectivity with maximum adsorption capacity of 92.3 $mg_{(Pb)}$ $g^{-1}_{(MIIP)}$ at 40 °C and pH 6.0. Also, this adsorbent has physical and chemical stability, low cost and simple-fast operation. A comparison of the presented work with the previously reports for lead extraction (Table 2) indicates that the proposed Pb-MIIP due to the use of n-benzoyl-n-phenyl hydroxylamine, provides better analytical merits of adsorption capacity and LOD. From the results obtained, it can be concluded that this polymer can be used as an excellent substrate for the adsorption of lead ion in real aqueous solutions.

5. References

[1] Kot, A., Namiesnik, J., The role of speciation in analytical chemistry, Trends Anal. Chem. 19 (2-3) (2000) 69-79. https://doi.org/10.1016/S0165-9936(99)00195-8.

[2] Chen, L., Xu, Z., Liu, M., Huang, Y., Fan, R., Su, Y., Hu, G., Peng, X., Lead exposure assessment from study near a lead-acid battery factory in China, Sci. Total Environ. 429 (2012) 191-198. https://doi.org/10.1016/j.scitotenv.2012.04.015.

[3] Qin, J., Wai, M., Oo, M., Wong, F., A feasibility study on the treatment and recycling of a wastewater from metal plating, J. Member. Sci. 208 (1-2) (2002) 213-221. https://doi.org/10.1016/S0376-7388(02)00263-6.

[4] Kristensen, P., Irgens, L. M., Daltveit, A. K., Andersen, A., Perinatal outcome among children of men exposed to lead and organic solvents in the printing industry, Am. J. Epidemiol. 137 (2) (1993) 134-144. https://doi.org/10.1093/oxfordjournals.aje.a116653.

[5] Hachem, C., Bocquillon, F., Zahraa, O., Bouchy, M., Decolourization of textile industry wastewater by the photocatalytic degradation process, Dyes Pigm. 49 (2) (2001) 117-125. https://doi.org/10.1016/S0143-7208(01)00014-6.

[6] Deng, L., Su, Y., Su, H., Wang, X., Zhu, X., Sorption and desorption of lead (II) from wastewater by green algae *Cladophora fascicularis*, J. Hazard. Mater. 143 (1-2) (2007) 220-225. https://doi.org/10.1016/j.jhazmat.2006.09.009.

[7] Yetilmezsoy, K., Demirel, S., Vanderbei, R. J., Response surface modeling of Pb(II) removal from aqueous solution by *Pistacia vera* L.: Box–Behnken experimental design, J. Hazard. Mater. 171 (1-3) (2009) 551-562. https://doi.org/10.1016/j.jhazmat.2009.06.035.

[8] Yetilmezsoy, K., Demirel, S., Artificial neural network (ANN) approach for modeling of Pb(II) adsorption from aqueous solution by Antep pistachio (*Pistacia Vera* L.) shells, J. Hazard. Mater. 153 (3) (2008) 1288-1300. https://doi.org/10.1016/j.jhazmat.2007.09.092.

[9] Markovac, J., Goldstein, G. W., picomolar concentrations of lead stimulate brain protein kinase C, Nature 334 (1988) 71-73. https://doi.org/10.1038/334071a0.

[10] Kunal, K. S., William, W., Sutherling, M. D., Role of lead in the central nervous system: effect on electroencephlography, evoked potentials, electroretinography, and nerve conduction, Neurodiagn. J. 55 (2) (2015) 107-121. https://doi.org/10.1080/21646821.2015.1043222.

[11] Tarley, C. R. T., Corazza, M. Z., Somera, B. F., Segatelli, M. G., Preparation of new ion-selective cross-

linked poly(vinylimidazole-coethylene glycol dimethacrylate) using a double-imprinting process for the preconcentration of Pb^{2+} ions J. Colloid. Interface Sci. 450 (2015) 254-263. https://doi.org/10.1016/j.jcis.2015.02.074.

[12] Behbahani, M., Hassanlou, P. G., Amini, M. M., Moazami, H. R., Abandansari, H. S., Bagheri, A., Hasanzadeh, S., Selective solid-phase extraction and trace monitoring of lead ions in food and water samples using new lead-imprinted polymer nanoparticles, Food Anal. Methods 8 (3) (2015) 558-568. https://doi.org/10.1007/s12161-014-9924-5.

[13] Clevenger, T., Novak, J., Recovery of metals from electroplating wastes using liquid-liquid extraction, J. Water Pollut. Control Fed. 55 (7) (1983) 984-989. https://www.jstor.org/stable/25042006.

[14] Zhou, Q., Bai, H., Xie, G., Xiao, J., Temperature-controlled ionic liquid dispersive liquid phase micro-extraction, J. Chromatogr. A. 117 (1) (2008) 43-49. https://doi.org/10.1016/j.chroma.2007.10.103..

[15] Duran, C., Gundogdu, A., Bulut, V. N., Soylak, M., Elci, L., Senturk, H. B., Tufekci, M., Solid-phase extraction of Mn(II), Co(II), Ni(II), Cu(II), Cd(II) and Pb(II) ions from environmental samples by flame atomic absorption spectrometry (FAAS), J. Hazard. Mater. 146 (1-2) (2007) 347-355. https://doi.org/10.1016/j.jhazmat.2006.12.029.

[16] Komjarova, I., Blust, R., Comparison of liquid–liquid extraction, solid-phase extraction and co-precipitation preconcentration methods for the determination of cadmium, copper, nickel, lead and zinc in seawater, Anal. Chim. Acta 576 (2) (2006) 221-228. https://doi.org/10.1016/j.aca.2006.06.002.

[17] Chen, J., Teo, K. C., Determination of cadmium, copper, lead and zinc in water samples by flame atomic absorption spectrometry after cloud point extraction, Anal. Chim. Acta 450 (1-2) (2001) 215-222. https://doi.org/10.1016/S0003-2670(01)01367-8.

[18] Haupt, K., Molecularly imprinted polymers in analytical chemistry, Analyst 126 (6) (2001) 747-756. https://doi.org/10.1039/B102799A.

[19] He, H., Xiao, D., He, J., Li, H., Dai, H., Peng, J., Preparation of a core–shell magnetic ion-imprintedpolymer *via* a sol–gel process for selectiveextraction of Cu(II) from herbal medicines Analyst 139 (10) (2014) 2459- 2466. https://doi.org/10.1039/C3AN02096G.

[20] Liu, Y., Liu, Z. Z., Wang, Y., Dai, J. D., Gao, J., Xie, J. M., Yan, Y. S., A surface ion-imprinted mesoporous sorbent for separation and determination of Pb(II) ion by flame atomic absorption spectrometry, Microchim. Acta 172 (3-4) (2011) 309-317. https://doi.org/10.1007/s00604-010-0491-1.

[21] Ghoohestani, S., Faghihian, H., Selective separation of Pb^{2+} from aqueous solutions by a novel imprinted adsorbent, Desalin. Water Treat. 57 (9) (2014) 1-10. https://doi.org/10.1080/19443994.2014.993718.

[22] Fan, H. T., Sun, X. T., Li, W. X., Sol–gel derived ion-imprinted silica-supported organic–inorganic hybrid sorbent for selective removal of lead(II) from aqueous solution, J. Sol-Gel Sci. Technol. 72 (1) (2014) 144-155. https://doi.org/10.1007/s10971-014-3436-z.

[23] Deng, H., Li, X., Peng, Q., Wang, X., Chen, J., Li, Y., Monodisperse magnetic single-crystal ferrite microspheres, Angew. Chem. 117 (18) (2005) 2842-2845. https://doi.org/10.1002/ange.200462551.

[24] Fang, C. L., Qian, K., Zhu, J., Wang, S., Lv, X., Yu, S. H., Monodisperse α-Fe_2O_3@SiO_2@Au core/shell nanocomposite spheres: synthesis, characterization and properties, Nanotechnology 19 (2008) 125601-125607. https://doi.org/10.1088/0957-4484/19/12/125601.

[25] Sarode, D. B., Ingle, S. T., Attarde, S. B., Formula establishment of colorless Pb(II) complex with N-benzoyl-N-phenyl hydroxyl amine (BPA) using atomic absorption spectroscopy, Indo. J. Chem. 12 (2012) 12-19. https://journal.ugm.ac.id/ijc/article/viewFile/21366/14071.

[26] Zhang, H. X., Dou, Q., Jin, X. H., Sun, D. X., Wang, D. D., Yang, T. R., Magnetic Pb(II) ion-imprinted polymer prepared by surface imprinting technique and its adsorption properties, Chem. Eng. J. 50 (6) (2015) 901-910. https://doi.org/10.1080/01496395.2014.978462.

[27] Zhang, M., Zhang, Z., Liu, Y., Yang, X., Luo, L., Chen, J., Yao, S., Preparation of core–shell magnetic ion-imprinted polymer for selective extraction of Pb(II) from environmental samples, Chem. Eng. J. 178 (2011) 443-450. https://doi.org/10.1016/j.cej.2011.10.035.

[28] Aboufazeli, F., Lotfi Zadeh Zhad, H. R., Sadeghi, O., Karimi, M., Najafi, E. Z., Novel ion imprinted polymer magnetic mesoporous silica nano-particles for selective separation and determination of lead ions in food samples, Food Chem. 141 (4) (2013) 3459-3465. https://doi.org/10.1016/j.foodchem.2013.06.062.

[29] Luo, X., Liu, L., Deng, F., Luo, S., Novel ion-imprinted polymer using crown ether as a functional monomer for selective removal of Pb(II) ions in real

environmental water samples, J. Mater. Chem. A 1 (28) (2013) 8280-8286. https://doi.org/10.1039/C3TA11098B.

[30] Girija, P., Beena, M., Sorption of trace amounts of Pb(II) ions on an ion imprinted interpenetrating polymer network based on alginic acid and crosslinked poly acryl amide, Sep. Sci. Technol. 49 (2014) 1053-1061. https://doi.org/10.1080/01496395.2013.866682.

[31] Sadeghi, O., Aboufazeli, H. R., Lotfi Zadeh Zhad, Karimi, M., Najafi, E., Determination of Pb(II) ions using novel ion-imprinted polymer magnetic nanoparticles: investigation of the relation between Pb(II) ions in cow's milk and their nutrition, Food Anal. Methods 6 (3) (2013) 753-760. https://doi.org/10.1007/s12161-012-9481-8.

[32] Ebrahimzadeh, H., Behbahani, M., A novel lead imprinted polymer as the selective solid phase for extraction and trace detection of lead ions by flame atomic absorption spectrophotometry: Synthesis, characterization and analytical application, Arab. J. Chem. 10 (2) (2017) 2499-2508. https://doi.org/10.1016/j.arabjc.2013.09.017.

[33] Behbahani, M., Bagheri, A., Taghizadeh, M., Salarian, M., Sadeghi, O., Adlnasab, L., Jalali, K., Synthesis and characterisation of nano structure lead (II) ion-imprinted polymer as a new sorbent for selective extraction and preconcentration of ultra trace amounts of lead ions from vegetables, rice, and fish samples, Food Chem. 138 (2-3) (2013) 2050-2056. https://doi.org/10.1016/j.foodchem.2012.11.042.

[34] Ebrahimzadeh, H., Asgharinezhad, A. A., Moazzen, E., Amini, M. M., Sadeghi, O., A magnetic ion-imprinted polymer for lead(II) determination: A study on the adsorption of lead(II) by beverages, J. Food Compos. Anal. 41 (2015) 74-80. https://doi.org/10.1016/j.jfca.2015.02.001.

[35] Sayar, O., Akbarzadeh Torbati, N., Saravani, H., Mehrani, K., Behbahani, A., Moghadam Zadeh, H.R., A novel magnetic ion imprinted polymer for selective adsorption of trace amounts of lead(II) ions in environment samples, J. Ind. Eng. Chem. 20 (5) (2014) 2657-2662. https://doi.org/10.1016/j.jiec.2013.10.052.

[36] Wei, S., Liu, Y., Shao, M., Liu, L., Wang, H., Liu, Y., Preparation of magnetic Pb(II) and Cd(II) ion-imprinted microspheres and their application in determining the Pb(II) and Cd(II) contents of environmental and food samples, RSC Adv. 4 (56) (2014) 29715-29723. https://doi.org/10.1039/C4RA01948B.

Eclética Química Journal, vol. 44, n. 4, 2019, 73-84
ISSN: 1678-4618
DOI: 10.26850/1678-4618eqj.v44.4.2019.p73-84